Interfacial Drag and Film Height for Vertical Annular Flow

New measurements are presented for film height and pressure drop for vertical gas-liquid annular flows. Improved methods for predicting the film height and interfacial friction factor are developed for situations in which the liquid film flow rate is known.

J. C. ASALI,
T. J. HANRATTY
Department of Chemical Engineering
University of Illinois
Urbana, IL
and
Paolo Andreussi
Instituto di Chemica Industriale Ed Applicata
Dipartimento di Ingegneria Chimica
Universita di Pisa
Pisa, Italy

SCOPE

When gas and liquid flow concurrently in a vertical pipe at high gas velocities, an annular configuration is reached for which a fraction of the liquid flows as a film along the wall and a fraction as droplets entrained in the gas. Frictional pressure drop in such a system is found to be much larger than for turbulent flow in a smooth pipe. This paper addresses the question of predicting the pressure drop and film height, m, if the liquid flow rate in the film, W_{LF}, is known.

Such measurements are usually interpreted by assuming that the roughened interface of the film causes the friction factor, f_i, to vary as the ratio of the film height to the pipe diameter, m/d_t, and that the relationship between W_{LF} and m is what would be calculated for a film velocity distribution that is the same as for a single phase turbulent flow. Henstock and Hanratty (1976) found that this approach was consistent with available measurements. However, they based their conclusions mainly on results for air-water flows upward in 3.14 and 3.45 cm pipes. Consequently there has been a need for results over a wider range of variables to test their proposed design relations.

This paper reports on research carried out for this purpose. Experiments were performed for vertical flow of air and a liquid up pipes with diameters of 2.29 and 4.2 cm. Water and water-glycerine solutions were used so that the viscosity was varied from 1.1 to 5.0 cp (mPa•s). Measurements were made of the film height, the film flow rate, and the pressure drop.

In discussing the results of these experiments a comparison is made with studies not included in the correlation of Henstock and Hanratty. These are the experiments for vertical downflows in 2.4 cm (Andreussi and Zanelli, 1978) and 3.18 cm pipes (Webb, 1970) and for vertical upflows in 0.95 cm (Cousins et al., 1965), 1.59 cm, and 3.18 cm (Shearer and Nedderman, 1965) pipes.

CONCLUSIONS AND SIGNIFICANCE

The correlations proposed by Henstock and Hanratty do not give satisfactory predictions either of the effect of pipe diameter on f_i or of the influence of film flow rate on film height.

For gas velocities greater than 25 m/s, $(f_i/f_s - 1)$ is found to vary with the film height made dimensionless with respect to the gas phase friction velocity and kinematic viscosity, m_g^+, rather than with the pipe diameter, m/d_t. This indicates that the interfacial shear between the gas and the liquid film is approximately independent of the size of the gas space. For low liquid flow rates the film height is described by

$$m^+ = 0.34Re_{LF}^{0.6}$$

rather than by the laminar flow relation. Here m^+ is the film height made dimensionless using the liquid phase friction velocity and kinematic viscosity.

On the basis of these results, improved methods, summarized in the last section, are developed to predict film height and pressure drop if W_{LF} is known. Thus the important ingredient needed to develop better design procedures for vertical annular gas-liquid flows is the prediction of the fraction of the liquid flowing as a liquid film.

INTRODUCTION

Two characteristic lengths can be defined for the air flow over the agitated liquid film. These are the tube diameter, d_t, and the friction length, $\nu_G(\tau_i/\rho_G)^{-1/2}$. If the wave surface can be characterized by a single length parameter proportional to the film height, m, then the frictional effect of the waves can be represented by two dimensionless groups, m/d_t and

$$m_g^+ = m(\tau_i/\rho_G)^{1/2}/\nu_G \qquad (1)$$

It has been argued that the wave surface on relatively thick films behaves analogously to a fully roughened sand surface (Hewitt and Hall-Taylor, 1970), so that the friction factor is defined by the relation $f_i \sim m/d_t$. For very thin films the waves are so small that $f_i = f_s$, where f_s is the friction factor for a smooth pipe.

The height of the film is usually related to the mass flow rate in the film, W_{LF}, by assuming that the film behaves the same as a single phase turbulent flow close to a wall (Henstock and Hanratty, 1976). In this approach, a dimensionless film thickness $m^+ = mv_c^*/\nu_L$ is defined, with $v_c^* = (\tau_c/\rho_L)^{1/2}$ and $\tau_c = \frac{2}{3}\tau_w + \frac{1}{3}\tau_i$. The wall stress, τ_w, depends on the interfacial stress, τ_i, and the body forces acting on the film. At high gas velocity $\tau_w \cong \tau_i$, Henstock and Hanratty found that m^+ is a function of the liquid film Reynolds number

$$m^+ = \gamma(Re_{LF}) \qquad (2)$$

where the function γ has been calculated to be

$$\gamma = [(0.707Re_{LF}^{0.5})^{2.5} + (0.0379Re_{LF}^{0.9})^{2.5}]^{0.4} \qquad (3)$$

It is noted that Eq. 3 gives the laminar flow relation for $Re_{LF} \rightarrow 0$ and the relation for a fully turbulent flow for $Re_{LF} \rightarrow \infty$. From Eqs. 2 and 3 one can calculate m if W_{LF} and v_c^* are known and develop a relation between f_i and W_{LF}, if $f_i \sim m/d_t$.

Henstock and Hanratty (1976) used the approach outlined above to examine the results of experimental studies in which the pressure drop, film height, and film flow rate were measured. They found reasonable agreement with Eqs. 2 and 3 and derived the following relations for m and for f_i for vertical upflows:

$$\frac{m}{d_t} = \frac{6.59F}{(f_i/f_s)^{1/2}} \qquad (4)$$

$$\frac{f_i}{f_s} = 1 + 1{,}400F \qquad (5)$$

$$f_s = 0.046Re_G^{-0.20} \qquad (6)$$

where F is a factor analogous to the Martinelli flow factor.

$$F = \frac{\gamma(Re_{LF})}{Re_G^{0.9}} \frac{\nu_L}{\nu_G} \sqrt{\frac{\rho_L}{\rho_G}} \qquad (7)$$

The analysis presented in this paper indicates a film height relation different from Eqs. 2 and 3. More importantly, it is found that the assumption of $(f_i/f_s - 1) \sim m/d_t$ does not correctly predict the effect of pipe diameter and that $(f_i/f_s - 1) \sim m_g^+$ is a better first-order representation of presently available results for gas velocities, U_G, greater than 25 m/s.

EXPERIMENT

The Flow Loop

The new experimental results presented in this paper were obtained in a loop containing three 9 m long vertical pipes that was designed by Asali (1984) for the study of the flow of air-liquid mixtures. Tests were conducted for upflows in plexiglass tubes with 4.2 and 2.29 cm I.D. These lines empty into a 15.2 cm dia. cylindrical manifold, 1.72 m long, which is connected to a separator to remove liquid from the air that discharges into the laboratory.

Water could be supplied to the system from a municipal water main, or a water-glycerine mixture could be recirculated with a centrifugal pump. The temperature of the liquid was controlled using a shell and tube heat exchanger. The liquid was introduced into a specially designed section through an annular slot around the pipe circumference.

Measurements were made of pressure drop, film thickness, and film flow rate. The results were reproducible, and the estimated errors were less than 5%.

Pressure Drop Measurements

Pressure drop was measured with two water manometers. Each manometer is connected to pressure taps in the test section and in the separator. The pressure drop is calculated as the difference in the readings of these two manometers. For the 4.2 cm tube, the upstream pressure tap is located 4.57 m from the entry section. There are two downstream taps, at 8.13 and 23.88 cm from the upstream tap. The 2.29 cm tube has taps at 3.96, 4.57, and 4.88 m from the entry section. All of these pressure taps were formed by drilling 1.59 mm holes through the pipe wall.

Dallman (1978), Laurinat (1982), and other investigators found that a small continuous purge was necessary in order to keep air bubbles from entering the leads to the pressure taps. We followed this procedure by using a carefully metered purge flow rate of less than 1% of the flow rate of the liquid film. Before making measurements all pressure tap leads were flushed several times at a high flow rate to remove air bubbles.

Film Thickness Measurements

For the range of gas and liquid flow rates covered in our experiments, the liquid film thicknesses varied from 200 to 30 μm. In addition to the difficulties associated with the measurement of such small thicknesses, there was also a possible problem associated with a nonuniform distribution of the liquid around the tube circumference. Therefore it was finally decided to take the precaution of measuring the mean thickness in a section of pipe rather than the local value.

The technique chosen involved the measurement of the conductance between two electrodes immersed in the liquid film. Detailed analyses of the performance of these probes are given by Coney (1973) and by Brown et al. (1978). The electrodes may either be flush with the wall or be wires protruding through the film. Flush probes are usually characterized by a nonlinear dependence of conductance on film thickness. However, when the electrodes are spaced far apart and the film is very thin, the response is well approximated by a linear relation. Flush-mounted probes were employed in our experiments because they do not introduce any disturbances into the film.

Two different electrode configurations were used. In the 4.2 cm pipe the electrodes are 3.175 cm stainless steel rods mounted flush with plugs that fitted into the pipe wall. The 2.29 cm pipe used ring electrodes that extended around the pipe circumference. The configuration of rods was simpler to construct but had the disadvantage of giving a smaller sensitivity to changes in film height.

The main difficulty in using a conductance cell to measure film thickness consists in suppressing undesired effects due to double layer and lead capacitance. These can almost be completely eliminated by an applied voltage of high enough frequency (100–500 kHz) that the double layer capacitance appears to be in parallel with the cell resistance and by increasing the conductivity of the liquid with the addition of an electrolyte. Since for thin films the conductance, G_E, is proportional to the product of the film thickness, m, and a conductivity coefficient, ϵ, it is possible to choose a value of ϵ that allows a strong enough output signal for any range of film thicknesses.

For both probe configurations the conductance varied only with the product $m\epsilon$. It was therefore not necessary to calibrate the probe for the thicknesses that are actually measured but only for a proper range of $m\epsilon$. The probes were calibrated by inserting plexiglass plugs of known diameter in the center of the test section and filling the free space with a liquid of known conductivity.

Local film thickness could be determined by measuring the conductance between pairs of the circular electrodes. Average film thicknesses around

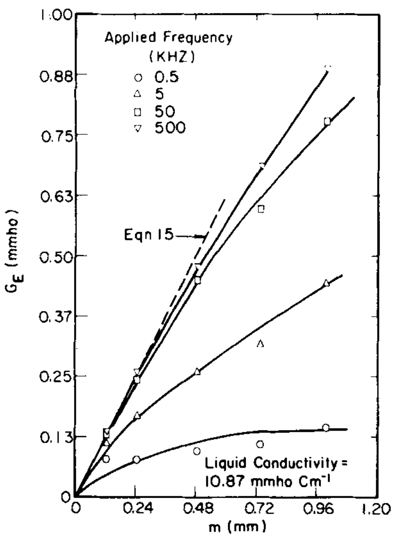

Figure 1. Calibration of circular electrodes used to measure film height in the 4.2 cm pipe.

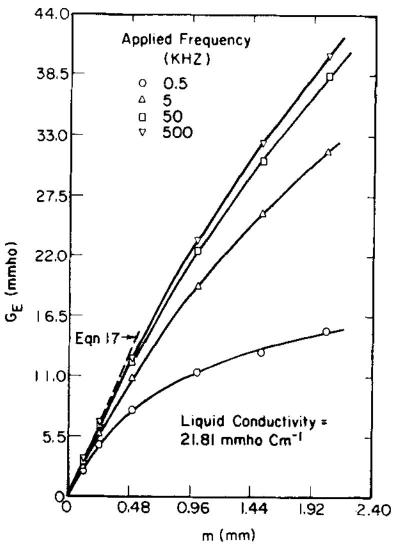

Figure 2. Calibration of the ring electrodes used to measure film height in the 2.29 cm pipe.

the circumference could be measured using a pair of circular electrodes located on opposite sides of the pipe or by using the pair of ring electrodes. The electrical behavior of the circular electrodes can be described by the method adopted by Brown et al. (1978). Asali (1983) used this method to show that the conductance between circular electrodes of radius, R_p, located in a flat wall that is immersed in a liquid of infinite extent and of depth, $m \ll R_p$, is given by

$$G_E = \frac{\pi \epsilon m}{\ln[(D_e - R_p)/R_p]} \tag{8}$$

where D_e is the distance between electrodes.

For electrodes facing each other on opposite sides of a circular tube of diameter d_t, the effect of the circular geometry must be taken in to account and

$$G_E = \frac{\pi \epsilon m}{\ln \left\{ \dfrac{\sin (R_p/d_t)}{\sin \left[\left(\dfrac{\pi d_t}{2} - R_p \right) \Big/ d_t \right]} \right\}} \tag{9}$$

In the present experiments, $R_p \ll d_t$, so Eq. 9 can be simplified to

$$G_E = \frac{\pi \epsilon m}{\ln(d_t/R_p)} \tag{10}$$

The theory for two-ring electrodes of length, l, separated by a distance, D_e, has been developed by Coney (1973):

$$G_E = \frac{l \epsilon \pi}{4 \ln 2 + \dfrac{\pi D_e}{m}} \tag{11}$$

If $D_e \gg m$, then

$$G_E = \frac{\pi d_t m \epsilon}{D_e} \tag{12}$$

since $l = \pi d_t$.

Calibration curves for pairs of circular and ring electrodes are compared with Eqs. 10 and 12 in Figures 1 and 2. It is seen that excellent agreement is obtained with films of thickness less than 200 μm at a frequency of 500 kHz. The experimentally determined proportionality constants of 0.95 and 12.4 for the circular and ring electrodes compare favorably with the values of 0.957 and 12.17 calculated from Eqs. 10 and 12.

Measurement of Film Flow Rate

The liquid film flow rate was calculated by subtracting the droplet flow rate from the total liquid flow rate. A pitot tube with a 3.175 mm O.D. and a 1.588 mm wall thickness was used to measure the droplet flux by withdrawing samples from the air stream. The total droplet flow rate was then calculated by performing an equal area integration (Perry and Chilton, 1973). The time-averaged film thickness defined the boundary of the core region for this integration.

Measurements of the entrained liquid taken close to the wall layer are subject to appreciable errors, since the probe may be sampling tips of large disturbance waves or liquid ligaments. At high values of liquid entrainment small errors in the measurement of liquid entrainment can cause appreciable errors in the calculation of the liquid film flow rate, which can be larger than 5%.

RESULTS

Flow Regimes

At low liquid flow rates the film is covered by long crested ripples having a steep front. Between these ripples the surface is smooth and the flow appears to be laminar. At sufficiently high liquid flow rates, roll waves appear on the film. These are observed as highly disturbed patches of fluid that extend around the circumference of the pipe (Shearer and Nedderman, 1965; Webb, 1970; Andreussi and Zanelli, 1978; Hall-Taylor et al., 1963; Hall-Taylor and Nedderman, 1968). These roll or disturbance waves move at much higher velocities than the ripples and are coherent in that they appear to keep their identity over a long length of pipe. This transition is accompanied by an atomization of liquid from the highly agitated roll wave crests, which are several times larger than the base film over which they move.

At large gas velocities the critical liquid film Reynolds number is independent of, or a weak function of, gas velocity, pipe diameter, gas density, and liquid viscosity. For gas velocities above 20 m/s, the ripple regime can approximately be identified with a limiting value of the liquid film Reynolds number of ~300 for vertical flows. This number decreases slowly with increasing liquid viscosity.

Film Height Results

Initial measurements of film height were made in the 4.2 cm pipe using configurations of circular electrodes. Measurements using all pairs of electrodes gave approximately the same time-

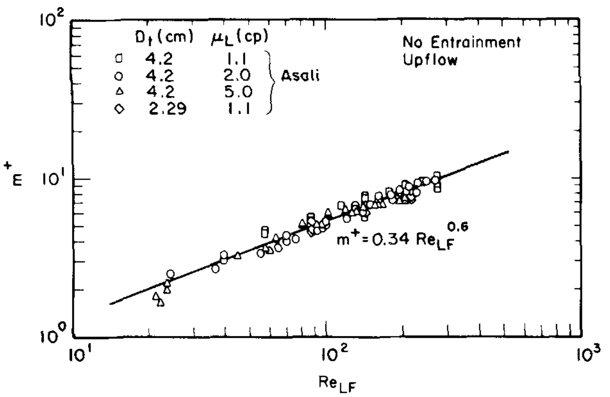

Figure 3. Film height measurements obtained at the University of Illinois at low enough film Reynolds numbers that liquid was not entrained in the gas.

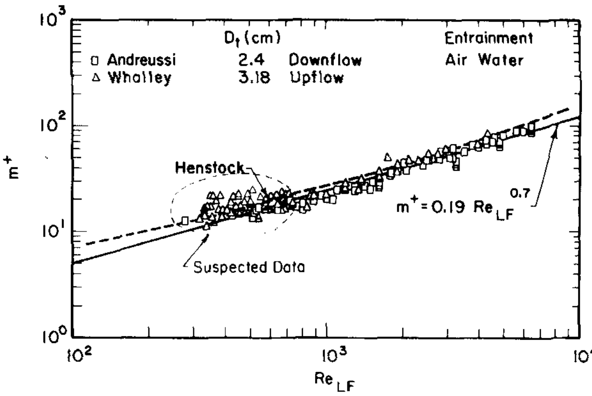

Figure 5. Film height measurements obtained by Whalley et al. (1973) and by Andreussi and Zanelli (1978).

averaged film thickness. This would indicate that the film was uniformly distributed around the circumference. The pair of ring electrodes was used in later measurements in the 2.29 cm pipe because of their greater sensitivity. All of the results reported in this paper were obtained with circular electrodes located on opposite sides of the 4.2 cm pipe and with the ring electrodes in the 2.29 cm test section.

Measurements of the film height taken under conditions that no entrainment existed in the gas phase are plotted, as suggested by Eq. 1, in Figure 3. The interfacial stress, used in this calculation, was calculated from pressure drop measurements in the fully developed region, by using the equation

$$\tau_i = -\frac{dP}{dx}\frac{(d_t - 2m)}{4} \tag{13}$$

The wall stress was calculated from a force balance on the liquid film

$$\tau_W = -\frac{d_t}{4}\frac{dP}{dx} \pm \rho_L g m \tag{14}$$

where the plus sign is used for downflow and the minus sign for upflow. The use of Eqs. 13 and 14 implies that contributions to the pressure gradient due to acceleration effects can be neglected. A consideration of the results indicates that this assumption is valid

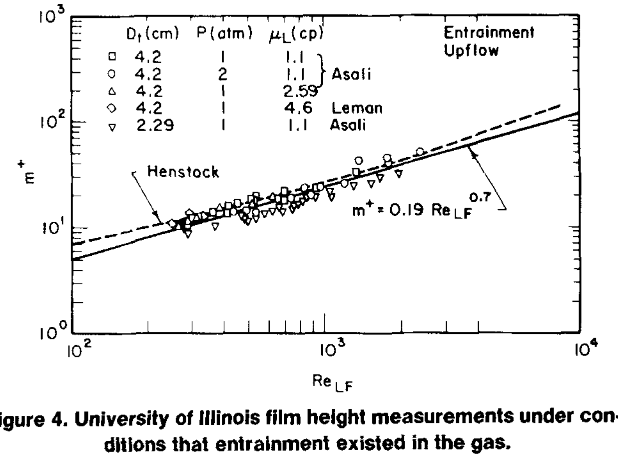

Figure 4. University of Illinois film height measurements under conditions that entrainment existed in the gas.

at the downstream end of the pipe, provided the gas velocity is less than 80 m/s.

The measurements for upward flow shown in Figure 3 are lower than the laminar flow relation and fit reasonably well with the equation

$$m^+ = 0.34 Re_{LF}^{0.6} \tag{15}$$

The measurements of film height under conditions that roll waves existed on the liquid film and that droplets were entrained in the gas are compared with the Henstock relation, Eqs. 2 and 3, in Figure 4. Reasonable agreement is obtained between the results obtained in the 4.2 cm pipe and the Henstock relation. No systematic effect of liquid viscosity is observed. However, a pipe diameter effect is noted in that the measurements with the 2.29 cm pipe are found to give smaller values of m^+ at a fixed Re_{LF} than the measurements in the 4.2 cm pipe.

Measurements by Andreussi and Zanelli (1978) and by Whalley et al. (1973) of film thickness for vertical flows with entrainment are plotted in Figure 5. The large disagreement between some of the measurements of Whalley et al. can be traced to errors in the measurements of W_{LF} (Asali, 1983) caused by the incomplete withdrawal of the wall film at low gas velocities. After ignoring these suspected data, approximate agreement with the Henstock relation is noted. However, there are significant differences, and these results suggest that the m^+ vs. Re_{LF} relation is more complicated than Eq. 3. For example, the data in Figure 5 seem to suggest a sudden change in the slope at $Re_{LF} \cong 1800$.

A comparison of Figures 4 and 5 shows that our results agree reasonably well with those in the literature. The spread in results obtained in this laboratory could reflect inaccuracies in the film flow rate, since, as already mentioned, the determination of this quantity can be subject to error at large droplet fluxes.

Friction Factors

An examination of friction factor measurements reveals that for large gas velocities f_i/f_s becomes approximately independent of gas velocity and of tube size for a given Re_{LF}. This is illustrated in Figure 6, where it is shown that f_i/f_s increases sharply for upflows at $U_G < 30$ m/s. This increase is probably associated with an approach toward a flooding condition where gravitational forces, as well as fluid drag, have a strong effect on the wave structures. Results for downward flows, reported by Andreussi and Zanelli (1978), show a decrease, rather than an increase, in f_i/f_s at small gas velocities for fixed Re_{LF}.

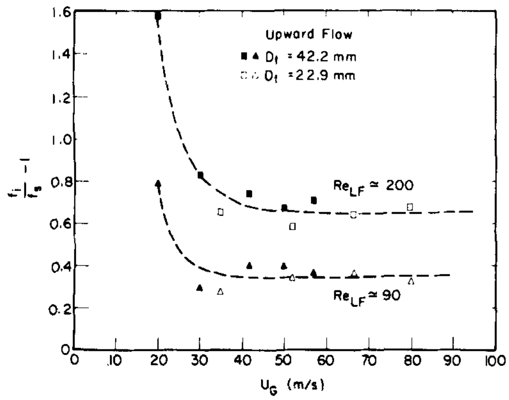

Figure 6. Effect of gas velocity on measurements of friction factors for upflows.

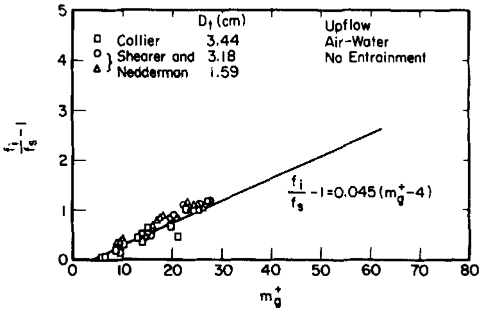

Figure 8. Measurements of friction factors obtained by Collier and Hewitt (1961) and Shearer and Nedderman (1965) for upflows with no entrainment.

These types of considerations suggest that for large gas velocities friction factor measurements should be correlated as a function of m_g^+, defined by Eq. 1. Figure 7 shows measurements for $U_G > 25$ m/s under conditions that there was no entrainment in the gas. These results fit quite well with relation

$$\frac{f_i}{f_s} - 1 = 0.045(m_g^+ - 4) \tag{16}$$

As shown in Figure 8, this relation also seems to fit friction factor results of Collier and Hewitt (1961), for a 3.44 cm pipe, and of Shearer and Nedderman (1965), for 1.59 and 3.18 cm pipes. Considerably higher values of the fraction factor are obtained at lower gas velocities, as shown in Figure 6. These measurements at $U_G \simeq 20$ m/s are fitted quite well by the relation

$$\frac{f_i}{f_s} - 1 = 0.065(m_g^+ - 4) \tag{17}$$

A clear-cut straight line relation between $f_i/f_s - 1$ and m_g^+ is also indicated by the downflow data of Andreussi and Zanelli (1978). However, a slightly higher value is obtained for the m_g^+ below which the surface may be considered smooth.

$$\frac{f_i}{f_s} - 1 = 0.045(m_g^+ - 5.9) \tag{18}$$

The data of Andreussi and Zanelli, of Charvonia (1959), and of Chien and Ibele (1964) are compared with Eq. 18 in Figure 9. Good agreement is noted.

The effect of entrainment on measurements of the friction factor is illustrated in Figure 10, where f_i/f_s is plotted against a Reynolds number based on the total liquid throughput. At low liquid Reynolds number, where no entrainment occurs, f_i/f_s is a function only of Re_L for a given fluid pair. In the entrainment region it is noted that larger values of f_i/f_s are obtained for the smaller gas Reynolds number. This can be explained, if the f_i/f_s is primarily a function of film Reynolds number, because an increase in the gas Reynolds number causes an increase in the amount of liquid entrained. Thus, for a fixed value of Re_L, the film Reynolds number will increase with decreasing gas velocity.

It is noted from Eq. 1 for fixed Re_L that m_g^+ increases with increasing liquid viscosity. The larger values of f_i/f_s at larger liquid viscosity, when comparisons are made at fixed Re_L, can therefore be explained if f_i/f_s depends primarily on m_g^+.

The above considerations and the success in using m_g^+ as a correlating parameter for measurements with no entrainment suggested that, as a first attempt, the friction factor measurements outside the ripple flow regime should be plotted, as shown in Figure 11. The curve shown on the graph is Eq. 16, derived for the ripple regime. A comparison of Eq. 16 with measurements for an upflow by Cousins et al. (1965) and by Whalley et al., (1973) is given in Figure 12. Cousins did not determine film heights, so the values of m_g^+ were calculated from his measurements of Re_{LF}, using Eqs. 2 and 3. Again, approximate agreement is noted, indicating that Eq. 16 represents the effects of pipe diameter over a range of almost 4.5 to 1.

A comparison of the large Re_{LF} downflow experiments of Andreussi and Zanelli (1978) with Eq. 16 is given in Figure 13. Again, approximate agreement is obtained between the experiments performed with and without entrainment.

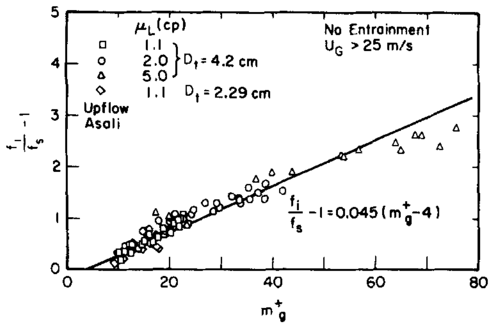

Figure 7. Measurements of friction factors obtained at the University of Illinois for flows with no entrainment at gas velocities greater than 25 m/s.

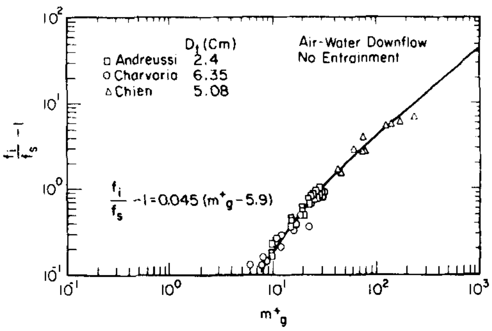

Figure 9. Measurements of friction factors made by Andreussi and Zanelli (1978), Charvonia (1959), and Chien and Ibele (1964) for downflows with no entrainment.

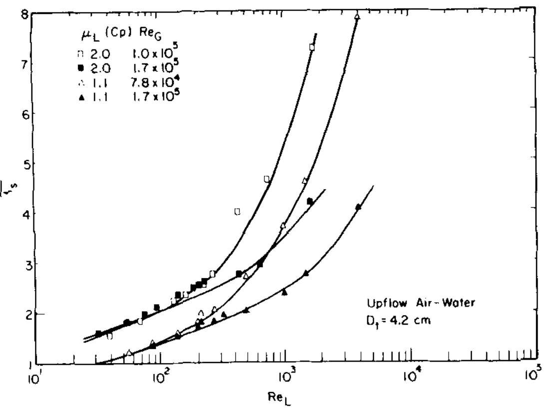

Figure 10. Effect of liquid and gas flow rates on friction factors measured for upflows.

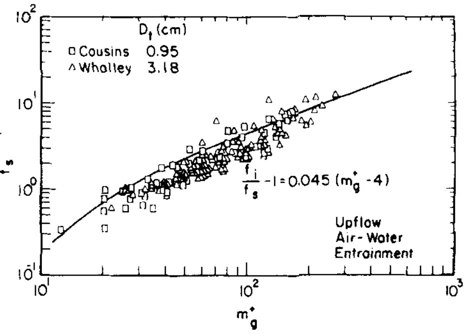

Figure 12. Measurements of friction factors for upflows with entrainment obtained by Cousins et al. (1965) and Whalley et al. (1973). A comparison with equation derived for no entrainment.

A comparison of Figures 11, 12, and 13 with Figures 7 and 8 indicates that an equation of the form $f_i/f_s \sim m_g^+$ does not describe the results for flows with entrainment as well as it does flows without entrainment. An examination of the results indicates for flows with entrainment that the friction factor is a function of Re_G, as well as m_g^+. Asali (1983) found that the group $m_g^+ Re_G^{-0.2}$ provides a better correlation of friction factor data than m_g^+. A reasonable representation of the results is obtained with the equation

$$\frac{f_i}{f_s} - 1 = 0.45(m_g^+ - 4)Re_G^{-0.2} \tag{19}$$

It is noted the parameter used in Eq. 19 gives an effect of gas Reynolds number that is intermediate between parameters m_g^+ and F, defined by Eqs. 1 and 7.

The results for downflow can be represented by the equation

$$\frac{f_i}{f_s} - 1 = 0.45(m_g^+ - 5.9)Re_G^{-0.2} \tag{20}$$

DISCUSSION

Film Heights

The most striking difference between the new measurements of film height presented in this paper and the correlation of Henstock and Hanratty is the relation of m^+ vs. Re_{LF} found for flows with no entrainment, Eq. 15. In the description of the experimental technique adopted for measuring film thickness, it has been pointed out that measurement of thicknesses below 200 μm is a difficult task. In fact, there are very few comprehensive studies with which the results can be compared. Further measurements would therefore be very useful to check our observation of a deviation from the laminar flow relation at low film Reynolds numbers.

For the present, there are no reasons to suspect that the results are affected by any systematic errors in the film thickness or shear stress measurements. In fact, we feel that the use of fluids more viscous than water enabled us to make more accurate measurements than would be possible if we had used only water. For example, at a liquid film Reynolds number of 50 and gas Reynolds number of 50,000 the film thickness of the water film in the 4.2 cm pipe is 170 μm; a glycerine solution with a viscosity of 5 cp gives a film with an average thickness of 380 μm at the same Re_{LF}.

Therefore we have tried to justify the large deviation from the laminar flow relation on theoretical grounds. A possible explanation can be found from the ripple structure of the gas-liquid interface. These ripples are characterized by a low value of the ratio of the amplitude (10–20 μm) and wavelength (2–3 mm). This implies that one might make a pseudosteady state assumption whereby the relation between the local height, h, and the local mass flow rate per unit width, Γ, is the same as for laminar film with a smooth surface:

$$(0.707)^2 \frac{4\Gamma}{\mu_L} = (hv_c^*/\nu_L)^2 \tag{21}$$

For these thin films

$$v_c^* \cong (\tau_i/\rho_L)^{1/2}$$

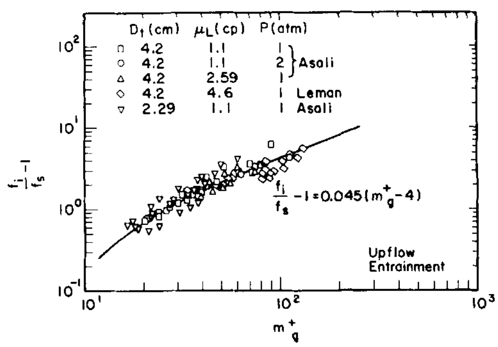

Figure 11. Measurements of friction factors obtained at the University of Illinois for annular flows with entrainment. A comparison with equation derived for no entrainment.

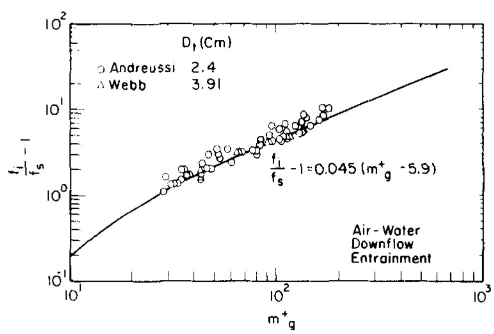

Figure 13. Measurements of friction factors for downflows with entrainment obtained by Andreussi and Zanelli (1978) and Webb (1970). A comparison with equation derived for flows without entrainment.

Since the average of $4\Gamma/\mu_L$ is the liquid film Reynolds number

$$(0.707)^2 Re_{LF} = \langle h^2 \tau_i \rangle / \rho_L \nu_L^2 \tag{22}$$

Now if the average of the product of h^2 and τ_i is greater than the product of the averages

$$\langle h^2 \tau_i \rangle > m^2 \langle \tau_i \rangle \tag{23}$$

the laminar flow relation

$$(0.707)^2 Re_{LF} = m^{+2} \tag{24}$$

would predict too large a value for m. This seems quite plausible, since $\langle h^2 \rangle > m^2$ and since it is expected that drag stress of the gas on the interface should be a maximum close to the wave crest (Thorsness et al., 1978).

Agreement is noted between our film height measurements with entrainment and those in the literature. The differences found between the measurements in the 2.29 and the 4.2 cm pipes might not be real and could reflect inaccuracies in entrainment measurements. This is something that will have to be checked in further experimentation. The data shown in Figures 4 and 5 are in approximate agreement with the relation presented by Henstock and Hanratty. However, there are significant differences. It appears that further analysis of this problem is needed. Since the accuracy of the theoretical basis of Eqs. 1 and 2 is uncertain, we have tended to use more convenient analytical forms to do practical calculations. For example the results in Figure 4 and 5 fit quite well with the relation

$$m^+ = 0.19 Re_{LF}^{0.7} \tag{25}$$

Friction Factors

The friction factor relation obtained for the ripple flow regime, with no entrainment, is found to be quite different from what was suggested by Henstock and Hanratty in that f_i/f_s varies with m_g^+, and not with m/d_t. If wave height scales with the film height, this type of correlation suggests that when the wave height is below a certain value the liquid surface may be considered smooth. Consistent with work reported by Hewitt and Hall-Taylor (1970), we find that this critical height is defined by the equation m_g^+ = constant. We get $m_{gC}^+ = 4$ for upflows and $m_{gC}^+ = 5.9$ for downflows, whereas Hewitt and Hall-Taylor give $m_{gC}^+ = 5$ for vertical flows.

The wave pattern in the ripple regime is quite different from that observed under conditions where atomization of the liquid film occurs. It is therefore quite surprising that the friction factor relations derived for the ripple regime also do a reasonably good job in the roll wave regime for a range of pipe diameters of 4.5 to 1 and a range of liquid viscosities of 4.6 to 1. However, it is noted that the accuracy of the correlation is not so good in the roll wall regime as it is in the ripple regime.

This inaccuracy appears to be partially associated with an effect of gas Reynolds number. Therefore we have tried to improve the correlation by arguing that at large m_g^+ the ratio of the friction factors, f_i/f_s, varies with $m_g^+ Re_G^{-.2}$. This employs an effect of gas Reynolds number that is intermediate between that found for the ripple regime and the F factor, defined by Eq. 7, suggested by Henstock and Hanratty.

DESIGN RELATIONS

Friction Factors for the Ripple Regime

For flows with liquid film Reynolds numbers less than what is required for the initiation of roll waves ($Re_{LF} < Re_{LFC}$), the following equations have been derived for the friction factor.

For upflows

$$\frac{f_i}{f_s} - 1 = C_1(m_g^+ - 4) \tag{26}$$

$$m_g^+ = 0.34 Re_{LF}^{0.6} \frac{\nu_L}{\nu_G}\left(\frac{\rho_L}{\rho_G}\frac{\tau_i}{\tau_C}\right)^{1/2} \tag{27}$$

For gas velocities greater than 25 m/sc, $C_1 = 0.045$ and $\tau_i/\tau_C \simeq 1$. For small gas velocities $C_1 > 0.045$.

For downflows, with $Re_{LF} < Re_{LFC}$

$$\frac{f_i}{f_s} - 1 = C_2(m_g^+ - 5.9) \tag{28}$$

Insufficient data are available for downflows to establish the dependency of m_g^+ on Re_{LF}, so it is tentatively recommended that m_g^+ be calculated from Eq. 27. For gas velocities greater than 25 m/s, $C_2 = 0.045$ and $\tau_i/\tau_C \simeq 1$. For small gas velocities $C_2 < 0.045$.

Friction Factors for the Roll Wave Regime

For the roll wave regime ($Re_{LF} > Re_{LFC}$), we recommend that the following equations be used to calculate friction factors.

For upflows

$$\frac{f_i}{f_s} - 1 = 0.45 Re_G^{-0.2}(m_g^+ - 4) \tag{29}$$

with

$$m_g^+ = 0.19 Re_{LF}^{0.7} \frac{\nu_L}{\nu_G}\left(\frac{\rho_L}{\rho_G}\frac{\tau_i}{\tau_C}\right)^{1/2} \tag{30}$$

For downflows

$$\frac{f_i}{f_s} - 1 = 0.45 Re_G^{-0.2}(m_g^+ - 5.9) \tag{31}$$

with m_g^+ defined by Eq. 30.

Film Heights

The following equations are recommended for calculating film heights for $Re_{LF} < 330$.

For upflow

$$\frac{m U_G f_s}{\nu_G} = \frac{1.414 m_g^+}{1 + C_1(m_g^+ - 4)^{1/2}} \tag{32}$$

and for downflow

$$\frac{m U_G f_s}{\nu_G} = \frac{1.414 m_g^+}{1 + C_2(m_g^+ - 5.9)^{1/2}} \tag{33}$$

with m_g^+ given as

$$m_g^+ = 0.34 Re_{LW}^{0.6} \frac{\nu_L}{\nu_G}\left(\frac{\rho_L}{\rho_G}\frac{\tau_i}{\tau_C}\right)^{1/2} \tag{34}$$

and

$$f_s = 0.046 Re_G^{-.20} \tag{35}$$

For $Re_{LF} > 330$, the film height relation is

$$\frac{m U_G (f_s)^{1/2}}{\nu_G} = \frac{1.414 m_g^+}{[1 + 0.45 Re_G^{-0.2}(m_g^+ - 4.0)]^{1/2}} \tag{36}$$

for upflow and is

$$\frac{m U_G (f_s)^{1/2}}{\nu_G} = \frac{1.414 m_g^+}{[1 + 0.45 Re_G^{-0.2}(m_g^+ - 5.9)]^{1/2}} \tag{37}$$

for downflow, with m_g^+ given by

$$m_g^+ = 0.19 Re_{LF}^{0.7} \frac{\nu_L}{\nu_G} \left(\frac{\rho_L}{\rho_G} \frac{\tau_i}{\tau_C}\right)^{1/2} \tag{38}$$

ACKNOWLEDGMENT

The authors acknowledge financial support from the Shell Oil Company, NSF CPE 72-20980, the NSF U.S.-Italy Cooperative Science Program, and the CNR of Italy.

NOTATION

- d_t = tube diameter
- D_e = distance of separation between ring electrodes or circular electrodes
- f_i = gas phase friction factor based on interfacial shear

$$f_i = \frac{\tau_i}{\frac{1}{2}\rho_G U_G^2}$$

- f_s = gas phase friction factor that would exist in a smooth tube, defined by Eq. 6
- F = dimensionless group containing flow rates and fluid properties, defined by Eq. 7
- g = acceleration of gravity
- G_E = conductance between two electrodes
- h = local film height
- l = length of ring electrodes
- m = averaged film height
- m^+ = dimensionless film height, $m^+ = m v_c^*/\nu_L$
- m_g^+ = dimensionless film height, defined by Eq. 1
- m_{gC}^+ = critical value of the dimensionless group, m_g^+, below which $f_i = f_s$
- P = perimeter wetted by the film
- Re_G = gas Reynolds number calculated as if the gas filled the whole tube, $Re_G = 4W_G/\mu_G P$
- Re_L = Reynolds number of the total liquid throughput, $Re_L = 4W_L/\mu_L P$
- Re_{LF} = Reynolds number of the liquid flowing in the wall layer, $Re_{LF} = 4W_{LF}/\mu_L P$
- Re_{LFC} = Reynolds number of the critical liquid flow rate for nonatomizing film, $Re_{LFC} = 4W_{LFC}/\mu_L P$
- R_P = radius of rod electrode
- U_G = mean axial gas velocity, $\dfrac{4W_G}{\pi(D-2m)^2\rho_G}$
- v_c^* = characteristic friction velocity, $v_c^* = (\tau_c/\rho_L)^{1/2}$
- V = potential of an electrode in a liquid layer
- W_L = total mass flow rate of the liquid in the units of mass per unit time
- W_{LF} = mass flow rate of the liquid in the wall layer
- W_{LFC} = critical mass flow rate of the liquid in the wall layer for nonatomizing film
- dp/dx = frictional pressure gradient

Greek Letters

- ϵ = conductivity coefficient of an electrolyte
- Γ = local mass flow rate per unit width
- γ = function of Re_{LF}, defined by Eq. 2
- ρ_G = gas density
- ρ_L = liquid density
- μ_G = gas viscosity
- μ_L = liquid viscosity
- ν_G = gas kinematic viscosity
- ν_L = liquid kinematic viscosity
- τ_c = characteristic shear stress, $\tau_c = \frac{2}{3}\tau_w + \frac{1}{3}\tau_i$
- τ_i = interfacial shear stress
- τ_w = wall shear stress

LITERATURE CITED

Andreussi, P., and S. Zanelli, "Downward Annular-Mist Flow of Air-Water Mixtures," Intern. Seminar, Dubrovrik, Yogoslavia, September 4–9 (1978).

Asali, J. C., "Entrainment in Vertical Gas-Liquid Annular Flows," Ph.D. Thesis, Univ. of Illinois, Urbana (1983).

Brown, R. C., P. Andreussi, and S. Zanelli, "The Use of Wire Probes for the Measurement of Liquid Film Thickness in Annular Gas-Liquid Flows," *Can. J. Chem., Eng.*, **56**, 754 (1978).

Charvonia, D. A., "A Study of the Mean Thickness of the Liquid Film and the Characteristics of the Interfacial Surface in Annular Two-Phase Flow in a Vertical Pipe," *Jet Propulsion Center Rept. No. I-59-1*, Purdue Univ. and Purdue Research Foundation, Lafayette, Ind. (1959).

Chien, S. F., and W. Ibele, "Pressure Drop and Liquid Film Thickness of Two-Phase Annular and Annular-Mist Flows," *J. Heat Transfer Trans. ASME*, **86**, 89 (1964).

Collier, J. G., and G. F. Hewitt, "Data on the Vertical Flow of Air-Water Mixtures in the Annular and Dispersed Flow Regions," *Trans. Inst. Chem. Eng.*, **39**, 127 (1961).

Coney, M. W. E., "The Theory and Application of Conductance Probes for the Measurement of Liquid Film in Two-Phase Flow," *J. Phys. E: Scientific Instruments*, **6**, 903 (1973).

Cousins, L. B., W. H. Denton, and G. F. Hewitt, "Liquid Mass Transfer in Annular Two-Phase Flow," *Atomic Energy Research Establishment Rept.* R4926 (1965).

Dallman, J. C., "Investigation of Separated Flow Model in Annular Gas-Liquid Two-Phase Flow," Ph.D. Thesis, Univ. of Illinois, Urbana (1978).

Hall-Taylor, N. S., G. F. Hewitt, and P. M. C. Lacey, "The Motion and Frequency of Large Disturbance Waves in Annular Two-Phase Flow of Air-Water Mixtures," *Chem. Eng. Sci.*, **18**, 537 (1963).

Hall-Taylor, N. S., and R. M. Nedderman, "The Coalescence of Disturbance Waves in Annular Two-Phase Flow," *Chem. Eng. Sci.*, **23**, 551 (1968).

Henstock, W. H., and T. J. Hanratty, "The Interfacial Drag and the Height of the Wall Layer in Annular Flows," *AIChE J.*, **22**(6), 990 (1976).

Hewitt, G. F., and N. S. Hall-Taylor, *Annular Two-Phase Flow*, Pergamon Press, Oxford (1970).

Laurinat, J. E., "Studies of the Effect of Pipe Size on Horizontal Annular Two-Phase Flows," Ph.D. Thesis, Univ. of Illinois, Urbana (1982).

Leman, G. W., "Effect of Liquid Viscosity in Two-Phase Annual Flow," M.S. Thesis, Univ. of Illinois, Urbana (1983).

Perry, R. H., and C. H. Chilton, *Chemical Engineers' Handbook*, 5th ed., 5 (1973).

Shearer, C. J., and R. M. Nedderman, "Pressure Gradient and Liquid Film Thickness in Co-current Upwards Flow of Gas/Liquid Mixtures: Application to Film-Cooler Design," *Chem. Eng. Sci.*, **20**, 671 (1965).

Webb, D., "Studies of the Characteristics of Downward Annular Two-Phase Flow. 3. Measurements of Entrainment Rate, Pressure Gradient, Probability Distribution of Film Thickness and Disturbance Wave Inception," *Atomic Energy Research Establishment Rept. R 6426* (1970).

Whalley, P. B., G. F. Hewitt, and P. Hutchinson, "Experimental Wave and Entrainment Measurements in Vertical Annular Two-Phase Fow," *Atomic Energy Research Establishment Rept. R 7521* (1973).

Manuscript received Nov. 7, 1983; revision received Aug. 7, 1984, and accepted Aug. 17.